

On the Vacuum energy of a Color Magnetic Vortex

M. BORDAG*

University of Leipzig, Institute for Theoretical Physics

Augustusplatz 10/11, 04109 Leipzig, Germany

October 26, 2018

Abstract

We calculate the one loop gluon vacuum energy in the background of a color magnetic vortex for $SU(2)$ and $SU(3)$. We use zeta functional regularization to obtain analytic expressions suitable for numerical treatment. The momentum integration is turned to the imaginary axis and fast converging sums/integrals are obtained. We investigate numerically a number of profiles of the background. In each case the vacuum energy turns out to be positive increasing in this way the complete energy and making the vortex configuration less stable. In this problem bound states (tachyonic modes) are present for all investigated profiles making them intrinsically unstable.

1 Introduction

Color magnetic vortices or center-of-group vortices play at present an important role in the discussion of possible mechanisms for confinement in QCD [1, 2, 3]. There are recent investigations of vortex like configurations in QED [4] and in QCD [5]. Given the actual interest in this topic we consider in the present paper the case of Abelian color magnetic vortices with arbitrary profile for $SU(2)$ and $SU(3)$ gluodynamics. Following the technique developed in [6] for a magnetic flux tube and earlier in [7] for a spherically symmetric background field we write down analytic expressions for the vacuum energy well suited for numerical investigation. Using zeta functional regularization we express the vacuum energy in terms of the Jost function of the related scattering problem, and by separating a piece of

*e-mail: Michael.Bordag@itp.uni-leipzig.de

the asymptotic expansion of the Jost function we obtain fast converging sums and integrals.

At present, several calculation schemes are known. The oldest and perhaps most intuitive one is to sum over phase shifts or, what is equivalent, over mode densities. For recent applications see [5] and [8]. This method is numerically demanding because of the oscillatory behavior of the phase shifts as function of the radial momentum. Another method that had been proposed in [7, 6] uses the Jost function and a momentum integration turned into the imaginary axis in this way avoiding oscillatory integrands (for a detailed description of these methods see also [9]). A completely different approach is that of [10, 11] using world line methods. Its main advantage is that it does not require separation of variables. Recently, this method was applied to a magnetic string and numerical results similar to those in [6] have been obtained (for a comparizon see [12]).

The issue of renormalization of vacuum energies has been much discussed in the past and different schemes are in use. Finally, all differences are settled by an appropriate normalization condition and the many schemes are different ways to the same destination. However, this is not always easy to see. Let us first consider theories with a massive quantum field, a spinor for instance. Here the mass of the field provides the opportunity to formulate the 'large mass' normalization condition stating the vacuum energy must vanish if this mass becomes large [13, 14]. This condition was initially formulated in connection with the Casimir effect for massive fields [15]. In [16] it was shown to be equivalent to the no tadpole normalization condition known in quantum field theory. This condition is directly related to the heat kernel expansion which is equivalent to the expansion of Greens functions in inverse powers of the mass [17]. It is also evident that this condition is in line with the charge renormalization appearing from vacuum energy calculations in QED. Another picture we observe with massless quantum fields. There is no such normalization condition causing, for instance, the known problems with the vacuum energy of a dielectric sphere [14]. However, in the present paper we are concerned with QCD and the vacuum fluctuation of the gluons. Although they are massless, in QCD there is the commonly accepted coupling constant renormalization involving the phenomenological quantity Λ_{QCD} . We will use this scheme. The only technical problem is that this scheme is frequently used together with the Pauli-Villars regularization while we use the zeta functional one. But the relation between both schemes can easily be written down, see Sect. 2.

The paper is organized as follows. In the next section we collect the general formulas for the color vortex and its vacuum energy. Following [5] we write down the condition for the minimum of the complete energy. In the two subsequent sections we consider in detail the finite and the asymptotic parts of the vacuum energy for the given configurations. In Sec. 5 the numerical results are represented. Sec. 6 contains a discussion and some technical details are given in the Appendix.

We hope to have represented all formulas in such detail, or given the corresponding references, that the reader is able to repeat the calculations.

2 The color magnetic vortex and its vacuum energy

We consider a non Abelian gauge field with standard action

$$S = \frac{1}{4g^2} \int d^4x \left(F_{\mu\nu}^a(x) \right)^2. \quad (1)$$

The corresponding potential, $A_\mu^a(x)$, is expanded around a background, $A_\mu^{a(\text{bg})}(x)$,

$$A_\mu^a(x) = A_\mu^{a(\text{bg})}(x) + A_\mu^{a(\text{qu})}(x), \quad (2)$$

where $A_\mu^{a(\text{qu})}(x)$ are the quantum fluctuations. The background is a center-of-group vortex, i.e., it is an Abelian static and cylindrically symmetric configuration. The corresponding color magnetic field is parallel to the third axis in both, color and space,

$$\vec{B}^a(x) = \delta^{a,3} \vec{e}_z \frac{\mu'(r)}{r}, \quad (3)$$

where $\mu(r)$ is a profile function, \vec{e}_z is the unit vector parallel to the z-axis and $\delta^{a,3}$ is the Kronecker symbol. The classical energy of this field meant as energy density per unit length with respect to the z-axis is

$$\mathcal{E}_{\text{class}} = \frac{\pi}{g^2} \int_0^\infty \frac{dr}{r} \mu'(r)^2. \quad (4)$$

The profile function will be chosen vanish at $r = 0$. Its first derivative must vanish too otherwise the classical energy is not finite. For $r \rightarrow \infty$ it must tend to a constant which determines the flux. We consider examples with $\mu(\infty) = 1$.

The fluctuation fields $A_\mu^{a(\text{qu})}(x)$ are quantized in a standard way. We use the background gauge condition as in [5] and have gluon and ghost contributions. The vacuum energy due to these fields is

$$\mathcal{E}_{\text{quant}} = \mathcal{E}_{\text{quant}}^{\text{gluon}} + \mathcal{E}_{\text{quant}}^{\text{ghost}}. \quad (5)$$

In general, a vacuum energy is given by

$$\mathcal{E}_{\text{quant}} = \pm \frac{1}{2} \sum_{(n)} e_{(n)}^{1-2s}, \quad (6)$$

where $e_{(n)}$ are the corresponding one particle energies and the sum over (n) is over all quantum numbers present for the given field. The parameter s is the

regularization parameter of the intermediate zeta functional regularization which we use. We have to take $s > \frac{3}{2}$ in the beginning and to put $s = 0$ in the end. We ignore the arbitrary parameter μ which is usually introduced in this scheme. The sign is +1 for gluons and -1 for ghosts. For both types of particles there is a sum over color and polarization. For the ghosts there is an additional factor of 2 because there are two fields, c and \bar{c} . In the considered background, variables separate in the equations of motion for the fluctuating fields. One can separate the dependence on the z-coordinate and the angular dependence in the plane perpendicular to the z-axis introducing p_z and the angular momentum ν ($\nu = 0, \pm 1, \pm 2, \dots$) accordingly. After that the one particle energies read

$$e_{(n)} = \sqrt{p_z^2 + \lambda_{\nu,n}^{(c,\lambda)^2}}, \quad (7)$$

where $\lambda_{\nu,n}^{(c,\lambda)}$ are the eigenvalues of the residual radial equation,

$$\left(-\frac{1}{r} \frac{\partial}{\partial r} r \frac{\partial}{\partial r} + \frac{(\nu - \alpha_c \mu(r))^2}{r^2} - \frac{2\alpha_c \beta_\lambda \mu'(r)}{r} \right) \phi_{\nu,n}^{(c,\lambda)}(r) = \lambda_{\nu,n}^{(c,\lambda)^2} \phi_{\nu,n}^{(c,\lambda)}(r). \quad (8)$$

Here we assume the radial quantum number n to be discrete, see below. This equation emerges after diagonalization in color space. The corresponding color eigenvalues are

$$\alpha_c = \begin{cases} \{0, -1, 1\} & \text{for SU(2)} \\ \{0, 0, -\frac{1}{2}, -\frac{1}{2}, \frac{1}{2}, \frac{1}{2}, -1, 1\} & \text{for SU(3)} \end{cases} \quad (9)$$

For the ghost field we have to put $\beta_\lambda = 0$ in Eq.(8). For the gluon the polarizations β_λ are

$$\beta_\lambda = \{0, 0, -1, 1\}. \quad (10)$$

In the vacuum energy, the two gluon polarizations with $\beta_\lambda = 0$ cancel the ghost contribution. So we are left with the two gluon polarizations $\beta_\lambda = \pm 1$ and no ghosts.

In the next step we integrate over p_z by means of

$$\int_{-\infty}^{\infty} \frac{dp_z}{2\pi} (p_z^2 + \lambda^2)^{\frac{1}{2}-s} = \lambda^{2(1-s)} \frac{\Gamma(s-1)}{2\sqrt{\pi}\Gamma(s-\frac{1}{2})} = \lambda^{2(1-s)} \frac{C_s}{4\pi s}$$

with $C_s = 1 + s(2 \ln 2 - 1) + \dots$ and arrive at

$$\mathcal{E}_{\text{quant}} = \frac{C_s}{2} \sum_{c,\lambda} \sum_{\nu=-\infty}^{\infty} \sum_n \lambda_{\nu,n}^{(c,\lambda)^2(1-s)}. \quad (11)$$

With this representation and equation (8) the whole problem is reduced to a number of scalar ones. Starting from here, and for pure technical convenience we introduce an auxiliary mass m by means of

$$\lambda_{\nu,n}^{(c,\lambda)} \rightarrow \left(\lambda_{\nu,n}^{(c,\lambda)^2} + m^2 \right)^{1/2} \quad (12)$$

with $m \rightarrow 0$ before the end of calculations.

It remains to transform the discrete sum over the radial quantum number n into an integral. As the initial problem is defined on the unbounded plane perpendicular to the z-axis this quantum number is continuous. We make it discrete by first imposing a large 'box', i.e., a cylinder at some large radius R with some boundary conditions. We follow [6] where this procedure is described in detail, but we discuss all subtle specifics of the given case. So, omitting all indices, let $\phi(r)$ be the regular solution of the radial equation on the whole axis. It is defined as that solution which at $r \rightarrow 0$ turns into the solution for $\mu(r) = 0$ which is simply the Bessel function $J_\nu(kr)$. For large r , $\phi(r)$ has the asymptotic expansion

$$\phi(r) \underset{r \rightarrow \infty}{\sim} \frac{1}{2} \left(f_\nu(k) H_\nu^{(2)}(kr) + \bar{f}_\nu(k) H_\nu^{(1)}(kr) \right). \quad (13)$$

The coefficients $f_\nu(k)$ and its complex conjugate are the Jost functions. The Hankel functions are also solutions of the radial equation (8) for $\mu(r) = 0$. However, we have to take into account $\mu(r) \underset{r \rightarrow \infty}{\sim} 1$ and should use the Hankel functions $H_{\nu-\alpha_c}^{(1,2)}(kr)$ instead. For the definition of the Jost function, this doesn't matter because the leading term in the asymptotic expansion of the Hankel functions for large argument doesn't depend on the index.

Following [6], for large R , the boundary condition $\phi(R) = 0$ defines the discrete eigenvalues $k \rightarrow \lambda_n$. This allows to write the sum over n as a contour integral encircling the spectrum with the logarithmic derivative of $\phi(R)$ generating the necessary poles. After that we tend r to infinity and drop a contribution which does not depend on the background (the so called Minkowski space contribution). In the heat kernel terminology this is to drop the coefficient a_0 's contribution. Finally turning the integration contour toward the imaginary axis we arrive at the representation

$$\sum_n \left(\lambda_n^2 + m^2 \right)^{1-s} = \frac{\sin \pi s}{-\pi} \int_m^\infty dk \left(k^2 - m^2 \right)^{1-s} \frac{\partial}{\partial k} \ln f_\nu(ik). \quad (14)$$

Putting these things together, we get for the vacuum energy (11),

$$\mathcal{E}_{\text{quant}} = \frac{C_s}{-8\pi} \sum_{c,\lambda} \sum_{\nu=-\infty}^{\infty} \int_m^\infty dk \left(k^2 - m^2 \right)^{1-s} \frac{\partial}{\partial k} \ln f_\nu^{(c,\lambda)}(ik), \quad (15)$$

where now $f_\nu^{(c,\lambda)}(ik)$ is the Jost function corresponding to Eq.(8) and we kept only first order corrections for $s \rightarrow 0$. This is a very convenient representation for the vacuum energy. The main advantage is that the integration goes over the imaginary axis avoiding oscillating functions. In addition we remark that bound states, if present in the spectrum, are included in this formula automatically¹. Bound states manifest themselves as zeros of the Jost function on the positive

¹This is discussed in detail in [18] and used in numerical examples in [19]

imaginary axis. If the binding energy κ_i is smaller than the mass m of the fluctuating field the corresponding poles of the logarithmic derivative are outside the integration region in Eq.(15) and the vacuum energy is real. In opposite case, for $m < \kappa_i$, the integration runs over the pole (it must be bypassed on the right) and an imaginary part appears. Using $\int \frac{dk}{k-i0} = i\pi$ we obtain

$$\Im \mathcal{E}_{\text{quant}} = \frac{-1}{8} \sum_{c,\lambda} \sum_{\nu} \sum_i (\kappa_i^2 - m^2), \quad (16)$$

where the sums go over those values of the quantum numbers for which a bound state is present. For instance, i is limited by $m < \kappa_i$. In our case we have $m = 0$ and any bound state contributes to the imaginary part of the vacuum energy. We note that the imaginary part does not contain ultraviolet divergences and so that we could put $s = 0$ here. The real part of the vacuum energy is then given by Eq.(15) taking the integration over k as principal value.

The vacuum energy given by Eq.(15) still contains known ultraviolet divergencies. Their structure can be best discussed in terms of the heat kernel coefficients. The contribution of the coefficient a_0 we already dropped. Due to the gauge invariance the coefficient a_1 is zero. The next coefficient is a_2 which is here given by

$$a_2 = \frac{-22N}{3}\pi \int \frac{dr}{r} \mu'(r)^2. \quad (17)$$

At once it is the last coefficient which contributes to the ultraviolet divergencies. By writing its contribution to the vacuum energy separately (for a derivation of the corresponding formula see [7]) we define by means of

$$\mathcal{E}_{\text{quant}} = \frac{-a_2}{32\pi^2} \left(\frac{1}{s} - 2 - 2 \ln \frac{m}{2} \right) + \mathcal{E}_{\text{quant}}^{\text{ren}} \quad (18)$$

the renormalized vacuum energy $\mathcal{E}_{\text{quant}}^{\text{ren}}$. In general, after separating the ultraviolet divergence, the remaining finite (in the limit of removing the regularization) part is not uniquely defined. In the form given here it contains contributions from the heat kernel coefficients a_n with numbers larger than 2 only. Because the heat kernel expansion provides an expansion in inverse powers, m^{4-2n} , of the mass of the fluctuating field, $\mathcal{E}_{\text{quant}}^{\text{ren}}$ goes to zero for $m \rightarrow \infty$. In problems with a massive fluctuating field we used this property as normalization condition defining in this way a unique renormalized vacuum energy [15, 13], see also [20]. For massless fields this does not work. In the case considered in this paper the underlying theory is QCD. Here the renormalization is done in the Pauli-Villars scheme by a redefinition of the bare coupling constant in Eq.(1) according to

$$\frac{1}{g^2} = \frac{11N}{24\pi^2} \ln \frac{M}{\Lambda_{\text{QCD}}}, \quad (19)$$

where M is the Pauli-Villars mass and N is the order of the gauge group, $SU(N)$. We denote for a moment the regularized vacuum energy by $\mathcal{E}_{\text{quant}}(s, m)$, indicating

the dependence on the regularization parameter s and on the mass m explicitly. In the Pauli-Villars scheme the vacuum energy is given by

$$\mathcal{E}_{\text{quant}}^{\text{PV}} = \mathcal{E}_{\text{quant}}(s, m) - \mathcal{E}_{\text{quant}}(s, M) \quad (20)$$

for $m \rightarrow 0$ and $M \rightarrow \infty$. Using the representation of the vacuum energy given by Eq.(18) as a result of the heat kernel decomposition we obtain

$$\begin{aligned} \mathcal{E}_{\text{quant}}^{\text{PV}} &= \frac{-a_2}{32\pi^2} \left(\frac{1}{s} - 2 - 2 \ln \frac{m}{2} \right) + \mathcal{E}_{\text{quant}}^{\text{ren}}(s, m) \\ &\quad - \frac{-a_2}{32\pi^2} \left(\frac{1}{s} - 2 - 2 \ln \frac{M}{2} \right) - \mathcal{E}_{\text{quant}}^{\text{ren}}(s, M). \end{aligned} \quad (21)$$

Here a number of contributions proportional to a_2 cancel, the pole term for instance², and in the limit we are left with

$$\mathcal{E}_{\text{quant}}^{\text{PV}} = \frac{-a_2}{16\pi^2} \ln M + \frac{a_2}{8\pi^2} \ln m + \mathcal{E}_{\text{quant}}^{\text{ren}}(m). \quad (22)$$

Here we have taken into account that $\mathcal{E}_{\text{quant}}^{\text{ren}}(s, M)$ vanishes for $M \rightarrow \infty$. Next, the contribution of $\ln M$ is canceled from the corresponding contribution from the classical energy by means of (19). Finally, in (22) the limit $m \rightarrow 0$ gives a finite result. This follows because $\mathcal{E}_{\text{quant}}$ as given by Eq.(18) is finite for a massless theory.

For the total energy we obtain

$$\begin{aligned} \mathcal{E} &= \mathcal{E}_{\text{class}} + \mathcal{E}_{\text{quant}}^{\text{PV}} \\ &= -\frac{11N}{24\pi} \ln \Lambda_{\text{QCD}} \int_0^\infty \frac{dr}{r} \mu'(r)^2 + \mathcal{E}_{\text{quant}}^{\text{renPV}} \end{aligned} \quad (23)$$

with the notation

$$\mathcal{E}_{\text{quant}}^{\text{renPV}} = \left(\frac{a_2}{16\pi^2} \ln m + \mathcal{E}_{\text{quant}}^{\text{ren}}(m) \right)_{|m=0} \quad (24)$$

for the vacuum energy renormalized in the Pauli-Villars scheme.

Eqs.(23) and (24) are the final answer for the complete energy of the vortex in QCD. It will be calculated for a number of profile functions in the subsequent sections. Because the vortex itself is unstable as its classical energy is positive a physical interest is in configurations lowering the complete energy. To find those a dimensional analysis can be made following [5]. First we note that the profile $\mu(r)$ is a dimensionless function of a variable with the dimension of a length. Therefore it must contain an intrinsic scale r_0 so that in fact we have to use

$$\mu \rightarrow \mu \left(\frac{r}{r_0} \right). \quad (25)$$

²Starting from here we can put $s = 0$ in $\mathcal{E}_{\text{quant}}^{\text{PV}}$.

Now we introduce the notation

$$A = \pi \int_0^\infty \frac{dr}{r} \mu'(r)^2 \quad (26)$$

to be used in Eq.(23). Note that A is dimensionless and a factor of $1/r_0^2$ had been taken out of the corresponding integral in Eq.(23). Next we note that $\mathcal{E}_{\text{quant}}^{\text{renPV}}$, Eq.(24) has for a background profile as given by Eq.(25) the following dependence on r_0 ,

$$\mathcal{E}_{\text{quant}}^{\text{renPV}} = -\frac{11N}{24\pi^2 r_0^2} A \ln r_0 + \frac{1}{r_0^2} \mathcal{E}_{\text{quant}}^{\text{renPV}}|_{r_0=1}. \quad (27)$$

This is for dimensional reasons. We introduce by means of

$$\ln B = -\frac{24\pi^2}{11NA} \mathcal{E}_{\text{quant}}^{\text{renPV}}|_{r_0=1} \quad (28)$$

the notation B , which allows to represent the complete energy in the form

$$\mathcal{E} = -\frac{11N}{24\pi^2} \frac{A}{r_0^2} \ln(r_0 \Lambda_{\text{QCD}} B). \quad (29)$$

After this rewriting the dependence of the complete energy on the scale r_0 is present in the shown places only. It is easy to find the minimum as a function of r_0 . After trivial calculation the minimum appears at

$$r_{0|_{\text{min}}} = \frac{1}{\Lambda_{\text{QCD}}} \frac{\sqrt{e}}{B}, \quad (30)$$

where e is the basis of the natural logarithms. The energy in the minimum is

$$\mathcal{E}_{|_{\text{min}}} = -\Lambda_{\text{QCD}}^2 \frac{11N}{24\pi^2} \frac{AB^2}{2e}. \quad (31)$$

This is the quantity to be compared for different profiles. Here the sign of the vacuum energy enters as follows. Primarily, the sign of the complete energy in the minimum, $\mathcal{E}_{|_{\text{min}}}$, is always negative. This is a consequence of the sign of a_2 resp. of the first coefficient of the beta function. Secondly, the sign of $\mathcal{E}_{\text{quant}}^{\text{renPV}}$ in Eq.(27) is dominated by $\ln r_0$ in the first contribution on the rhs of Eq.(27) and depends in this way on the scale. The second contribution, $\mathcal{E}_{\text{quant}}^{\text{renPV}}|_{r_0=1}$, may be positive or negative which will be a result of the calculations for a specific profile $\mu(r)$. If the sign of $\mathcal{E}_{\text{quant}}^{\text{renPV}}|_{r_0=1}$ is positive (negative) we have $B < 1$ ($B > 1$) and this contribution increases (decreases) the complete energy. At once, B influences the core radius in the minimum, $r_{0|_{\text{min}}}$, making it larger (smaller) for $B > 1$ ($B < 1$). We will see below in all considered examples we have $B > 1$. After this discussion of the scale dependence in all following calculations (Sec. 3 and 4) we put $r_0 = 1$.

3 The finite part of the vacuum energy

The regularized vacuum energy is given by Eq.(15) and we need to represent it in the form of Eq.(18), i.e we need to separate the pole part in s . Eq.(15) is well defined for $s \geq \frac{3}{2}$ and we need to perform the analytic continuation to $s = 0$. In order to do that we add and subtract a piece of the uniform asymptotic expansion of the logarithm of the Jost function which we define by

$$\ln f_\nu(ik) \sim \ln f_\nu^{\text{as}}(ik) + O\left(\frac{1}{\nu^4}\right) \quad (32)$$

for $\nu, k \rightarrow \infty$ with $z \equiv \frac{k}{\nu}$ fixed. In this way we represent

$$\mathcal{E}_{\text{quant}} = \mathcal{E}^{\text{f}} + \mathcal{E}^{\text{as}} + \mathcal{E}_0^{\text{f}} + \mathcal{E}_0^{\text{as}} \quad (33)$$

with

$$\mathcal{E}^{\text{f}} = \frac{-1}{8\pi} \sum_{c,\lambda} \sum_{\substack{\nu=-\infty \\ \nu \neq 0}}^{\infty} \int_m^{\infty} dk \left(k^2 - m^2 \right) \frac{\partial}{\partial k} \left(\ln f_\nu^{(c,\lambda)}(ik) - \ln f_\nu^{(c,\lambda)\text{as}}(ik) \right), \quad (34)$$

and

$$\mathcal{E}^{\text{as}} = \frac{C_s}{-8\pi} \sum_{c,\lambda} \sum_{\substack{\nu=-\infty \\ \nu \neq 0}}^{\infty} \int_m^{\infty} dk \left(k^2 - m^2 \right)^{1-s} \frac{\partial}{\partial k} \ln f_\nu^{(c,\lambda)\text{as}}(ik), \quad (35)$$

where we in the Jost functions again indicated the dependence on color and on polarisation. In Eq.(34) we have put $s = 0$ because there the sum and the integral are convergent. This is ensured by the choice of the asymptotic part of the Jost function. It can be checked that both, the integral and the sum are made convergent by subtracting the uniform asymptotic expansion. This fact is non trivial and doesn't hold for any background potential. For instance, it can be shown that for a $\mu(r)$ with a non vanishing first derivative in $r = 0$ the integral is not convergent. But in that case the classical part of the energy, Eq.(4), is infinite. This we do not consider.

In Eqs. (34) and (35) we left out the contribution from the orbital momentum $\nu = 0$ because it needs a separate treatment. Here we define the asymptotic part of the Jost function as that for large argument k ,

$$f_0(ik) \sim f_0^{\text{as}}(ik) + O\left(\frac{1}{k^4}\right) \quad (36)$$

for $k \rightarrow \infty$. Accordingly we have

$$\mathcal{E}_0^{\text{f}} = \frac{-1}{8\pi} \sum_{c,\lambda} \int_m^{\infty} dk \left(k^2 - m^2 \right) \frac{\partial}{\partial k} \ln \left(f_0^{(c,\lambda)}(ik) - f_0^{(c,\lambda)\text{as}}(ik) \right), \quad (37)$$

and

$$\mathcal{E}_0^{\text{as}} = \frac{C_s}{-8\pi} \sum_{c,\lambda} \int_m^{\infty} dk \left(k^2 - m^2 \right)^{1-s} \frac{\partial}{\partial k} \ln f_0^{(c,\lambda)\text{as}}(ik). \quad (38)$$

Again, in Eq.(37) we could set $s = 0$ because the integral over k is convergent.

The asymptotic expansion of the Jost function can be obtained in the same way as in Ref.[7] and in Ref.[6] from iterating the Lippmann-Schwinger equation. While in [7] the background was scalar only two iterations were needed while in [6] for a vector background four had to be included. In the present case the background is a vector, hence we need four iterations. In [6] the quantum field was a spinor one and here we have a vector field. So we need to modify the formulas of [6] to some extend. The basic formula is the Lippmann-Schwinger equation which appears if rewriting the wave equation (8) as an integral equation (we drop the color and polarization indices for a moment),

$$\phi(r) = \phi^0(r) + \frac{\pi}{2i} \int_0^r \frac{dr'}{r'} \left(J_\nu(kr) H_\nu^{(1)}(kr') - J_\nu(kr') H_\nu^{(1)}(kr) \right) P(r') \phi(r') \quad (39)$$

with the 'perturbation operator'

$$P(r) = -2\alpha_c \mu(r) + \alpha_c^2 \mu(r)^2 - 2\alpha_c \beta_\lambda r \mu'(r) \quad (40)$$

and the choice $\phi^0(r) = J_\nu(kr)$ for 'free' solution which just makes $\phi(r)$ defined by Eq.(39) the regular solution. From considering this equation for $r \rightarrow \infty$ and comparing with Eq.(13) the following representation for the Jost function can be obtained,

$$f_\nu(k) = 1 + \frac{\pi}{2i} \int_0^\infty \frac{dr}{r} H_\nu^{(1)}(kr) P(r) \phi(r). \quad (41)$$

The next steps go exactly as in Ref.[6]. The logarithm of the Jost function which is the quantity we are interested in can be represented as given by Eqs.(32)-(35) in [6] with obvious substitutions. In these formulas one has to turn to imaginary k . After that the modified Bessel functions entering have to be substituted by their well known uniform asymptotic expansion and the integrations have to be performed by the saddle point method keeping all the contributions up to the necessary order. This is a quite lengthy calculation which is best performed by a computer algebra package to avoid errors. The result is a representation of the asymptotic expansion of the logarithm of the Jost function of the form

$$\ln f_\nu^{\text{as}}(ik) = \sum_{n=1}^3 \sum_{j=n}^{3n} \int_0^\infty \frac{dr}{r} X_{nj} \frac{t^j}{\nu^n} \quad (42)$$

with

$$t = \frac{1}{\sqrt{1 + (zr)^2}} \quad (43)$$

($z = k/\nu$). The coefficients X_{nj} are local functions of $\mu(r)$ and its derivatives. They are listed in the Appendix. It turns out that this is not the most convenient

form. It is possible to integrate in Eq.(42) by parts so that all contributions become proportional at last to one derivative of $\mu(r)$. In particular this speeds up the convergence of the integrals at $r \rightarrow \infty$ which later on must be taken numerically. After integrating by parts the formula looks essentially the same except that the coefficients are different. We denote them by Z_{nj} so that we obtain $\ln f_\nu^{\text{as}}(ik)$ in the form

$$\ln f_\nu^{\text{as}}(ik) = \sum_{n=1}^3 \sum_{j=n}^{3n} \int_0^\infty \frac{dr}{r} Z_{nj} \frac{t^j}{\nu^n}, \quad (44)$$

where the new coefficients are listed in the Appendix too.

For zero orbital momentum, $\nu = 0$, we need the asymptotic expansion of the Jost function for large argument. It can be obtained from Eqs.(32) and (33) in Ref.[6] by inserting there the asymptotic expansion of the Bessel functions for large argument. This is much easier than in the case of the uniform asymptotic expansion. This allows us to present these formulas here in order to illustrate the method. From the mentioned equations in [6] we have

$$\ln f^{(1)} = \int_0^\infty \frac{dr}{r} I_\nu(kr) K_\nu(kr) P(r) \quad (45)$$

and

$$\ln f^{(2)} = \int_0^\infty \frac{dr}{r} K_\nu^2(kr) P(r) \int_0^\infty \frac{dr'}{r'} I_\nu^2(kr') P(r'). \quad (46)$$

In Eq.(45) we use the expansion

$$I_\nu(kr) K_\nu(kr) = \frac{1}{2kr} + \frac{1}{16(kr)^3} + \dots \quad (47)$$

In Eq.(46) it is sufficient to use the leading order from the expansion of the Bessel functions, $K_\nu^2(kr) = \exp(-2kr)/(2kr) + \dots$ and $I_\nu^2(kr) = \exp(2kr)/(2kr) + \dots$ and to take the integral over r' by the saddle point method to leading order. The result is

$$\ln f^{(2)} = -\frac{1}{8k^3} \int_0^\infty \frac{dr}{r} P(r)^2. \quad (48)$$

Taking both contributions together we define

$$\ln f_0^{\text{as}}(ik) = \int_0^\infty \frac{dr}{r} \left\{ \frac{P(r)}{2kr} + \frac{1}{(k^2 + 1)^{3/2}} \left(\frac{P(r)}{16r^3} - \frac{P^2(r)}{8r^3} \right) \right\}. \quad (49)$$

Here we substituted $1/k^3$ by $1/(k^2 + 1)^{3/2}$. This does not change the asymptotics to the given order but avoids problems with the integration over k at the origin in Eq.(37) when we put $m = 0$ later on.

Now, in order to calculate the finite parts of the vacuum energy we need a method to calculate the Jost function numerically. Here we follow the ideas of Ref.[19] with necessary modifications. The Jost function $f_\nu(k)$ is defined by Eq.(13). We start from defining a new function $f_\nu(k, r)$ by means of

$$\phi(r) = \frac{1}{2} \left(f_\nu(k, r) H_{\nu-\alpha_c}^{(2)}(kr) + \bar{f}_\nu(k, r) H_{\nu-\alpha_c}^{(1)}(kr) \right). \quad (50)$$

From the definition, Eq.(13), it is clear that

$$f_\nu(k, r) \underset{r \rightarrow \infty}{\sim} f_\nu(k). \quad (51)$$

The speed of convergence depends on how fast the potential $\mu(r)$ approaches its value at infinity. It can be shown that the derivative of $f_\nu(k, r)$ with respect to r is proportional to $\mu(r) - 1$.

For a numerical calculation of the wave function $\phi(r)$ we can use the radial equation, Eq.(8) and solve it with some Runge-Kutta procedure. For this end we need initial conditions at $r = 0$. Here it is necessary to introduce a new function by means of

$$\phi(r) = \left(\frac{kr}{2} \right)^\nu \frac{\varphi(r)}{\Gamma(\nu + 1)}. \quad (52)$$

Given $\phi(r)$ is the regular solution it behaves for $r \rightarrow 0$ like the Bessel function $J_\nu(kr)$ and the introduced function $\varphi(r)$ is finite at the origin,

$$\varphi(0) = 1. \quad (53)$$

As the second initial value we need the derivative of $\varphi(r)$ in $r = 0$. Because $\mu(r)$ vanishes there together with its first derivative,

$$\varphi'(0) = 0 \quad (54)$$

holds.

In the numerical calculations we used Mathematica and the build in function **NDSolve**. Here it is useful to turn to a system of first order equation by means of

$$\begin{aligned} \varphi'(r) &= \psi(r), \\ \psi'(r) &= -\frac{2\nu+1}{r}\psi(r) + \left(-\frac{2\alpha_c\nu\mu(r)}{r} + \frac{\alpha_c^2\mu(r)^2}{r^2} - \frac{2\alpha_c\beta_\lambda\mu'(r)}{r} - k^2 \right) \varphi(r). \end{aligned}$$

Also it is necessary to move the starting point of the procedure away from $r = 0$ because otherwise **NDSolve** tries to divide $\varphi'(0)$ by $r = 0$. The initial data shifted by a small amount Δ can be obtained from a decomposition of the equations in powers of r and in the lowest nontrivial order we get

$$\begin{aligned} \varphi(\Delta) &= 1, \\ \psi(\Delta) &= \Delta \mu_2 \end{aligned} \quad (55)$$

with $\mu_2 = \mu''(r)|_{r=0}$. Now it remains to express the Jost function, $f_\nu(k, r)$, from Eq.(50) in terms of the functions $\varphi(r)$ and $\psi(r)$. In addition we need the Jost function for imaginary argument. So we have to substitute $k \rightarrow ik$ in the above equations. An easy calculation gives

$$f_\nu(ik, r) = \frac{(kr/2)^\nu}{\Gamma(\nu + 1)} \left(r\psi(r)K_{\nu-\alpha}(kr) + \varphi(r) \left(kK_{\nu+1-\alpha}(kr) + \frac{\alpha}{r}K_{\nu-\alpha}(kr) \right) \right), \quad (56)$$

where $K_{\nu-\alpha}(kr)$ are modified Bessel functions. In the process of solving the equations using `NDSolve` the true Jost function is approached quite fast. In all considered examples it was sufficient to take $r = 10$.

By means of Eqs.(34) and (44) we have all we need for a numerical calculation of \mathcal{E}^f . In the actual calculations we used Eq.(34) in a modified form. We integrated by parts and change the integration variable from k to $z = k/\nu$. Finally, we put $m = 0$ because here this auxiliary mass is no longer needed. In this way the formula reads

$$\mathcal{E}^f = \frac{1}{2\pi} \sum_{c,\lambda} \sum_{\substack{\nu=-\infty \\ \nu \neq 0}}^{\infty} \nu^2 \int_0^\infty dz z \left(\ln f_\nu^{(c,\lambda)}(i\nu z) - \ln f_\nu^{(c,\lambda)\text{as}}(i\nu z) \right). \quad (57)$$

Here a number of comments are in order. First, in Eq.(56) is written for positive orbital momenta. This is sufficient because the negative ones can be obtained by changing the signs of α_c and β_λ as can be seen from Eq.(8). Second, there are cancellations between contributions with different signs of the orbital momenta. For instance, there are even powers in $1/\nu$ in the uniform asymptotic expansion. They cancel³. Also, contributions odd in β_λ cancel in the sum over the polarizations. For large ν , because of the definition Eq.(32) the difference of the two logarithms in Eq.(57) decreases as $1/\nu^4$. In fact, under the sum over color and polarizations it decreases as $1/\nu^5$. As a function of z it decreases as $1/z^4$. The integral over z decreases as $1/\nu^5$. So the convergence is quite well. For instance, it is sufficient to take a few orbital momenta to achieve a precision of several digits.

In order to represent the results we introduce the notations

$$\mathcal{E}^f(\nu, z) = \frac{z}{\pi} \sum_{c,\lambda} \left(\ln f_\nu^{(c,\lambda)}(i\nu z) - \ln f_\nu^{(c,\lambda)\text{as}}(i\nu z) \right) \quad (58)$$

where the factor of 2 resulting from the two signs of the orbital momentum was taken into account and

$$\mathcal{E}^f(\nu) = \int_0^\infty dz z \mathcal{E}^f(\nu, z) \quad (59)$$

³This is taken into account already in the coefficients X_{nj} and Z_{nj} listed in the Appendix.

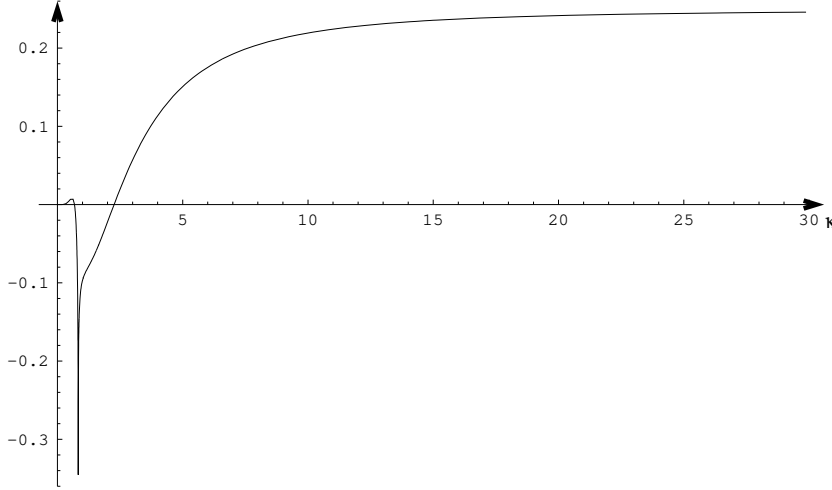


Figure 1: The s-wave contribution, $\mathcal{E}_0^f(k)$, multiplied by k^4 .

where the factor of 2 results from the two sign of the orbital momentum so that

$$\mathcal{E}^f = \sum_{\nu=1}^{\infty} \nu^2 \mathcal{E}^f(\nu) \quad (60)$$

holds.

In a similar way the contribution of the s-wave ($\nu = 0$) can be treated. Actually, it is much easier because there is only one integration and no sum. We put $m = 0$ in Eq.(37), integrate by parts and write it in the form

$$\mathcal{E}_0^f = \int_0^{\infty} dk \ k \ \mathcal{E}_0^f(k) \quad (61)$$

with

$$\mathcal{E}_0^f(k) = \frac{k}{4\pi} \sum_{c,\lambda} \ln \left(f_0^{(c,\lambda)}(ik) - f_0^{(c,\lambda)as}(ik) \right). \quad (62)$$

As an example let us consider the profile

$$\mu(r) = \tanh^2(r). \quad (63)$$

It vanishes for $r \rightarrow 0$ together with its first derivative and it approaches its value at infinity exponentially fast.

Fig. 1 shows the function $\mathcal{E}_0^f(k)$ multiplied by k^4 . It can be seen that its decrease is confirmed by the numerical results.

In Fig. 2 the functions $\mathcal{E}^f(\nu, z)$ multiplied by $z^3 \nu^{4.5}$ are plotted showing that the expected behavior for large z is confirmed by the numerical evaluation. The factor z^3 is taken to demonstrate the fast asymptotic decrease and the factor $\nu^{4.5}$

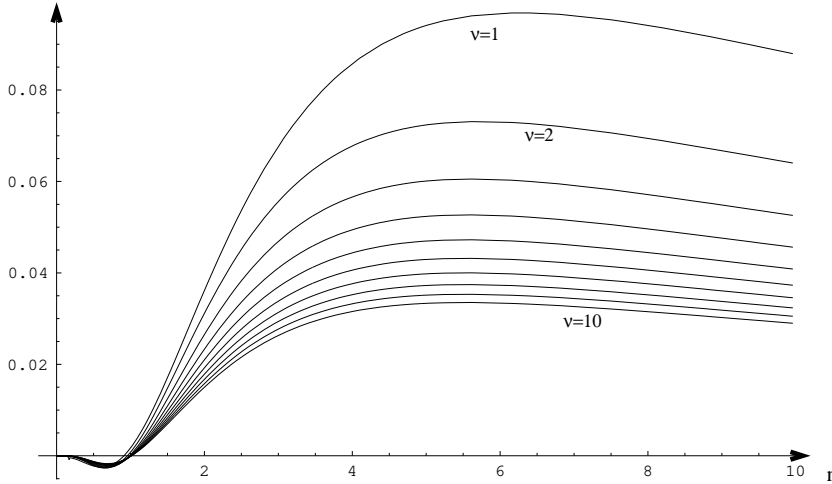


Figure 2: The functions $\mathcal{E}^f(\nu, z)$ multiplied by $z^3\nu^{4.5}$ for the first ten orbital momenta.

in order to have the curves for all orbital momenta ($\nu = 1, \dots, 10$) to fit into one figure.

In Fig. 3 the contributions $\mathcal{E}^f(\nu)$ from the higher orbital momenta ($\nu = 2, \dots, 10$) to the vacuum energy multiplied by ν^5 are shown. The corresponding sum in Eq.(61) is fast converging and in fact it is sufficient to take some few first orbital momenta only. As an illustration we show the corresponding numbers,

$$\begin{aligned} \mathcal{E}_0^f &= -0.0482214, \\ \nu &= \quad 1 \quad \quad \quad 2 \quad \quad \quad 3 \quad \quad \quad 4, \\ \nu^2 \mathcal{E}^f(\nu) &= \quad -0.00587755 \quad -0.00039075 \quad -0.000156122 \quad -0.0000753351. \end{aligned} \quad (64)$$

It should be remarked that the observed decrease of the subtracted Jost functions is a strong check confirming that the formulas for both, the Jost function itself and for its asymptotic expansions, are correct. This is because these formulas are obtained in completely different ways. The first one is a numerical solution of the differential equation and the second one results from the asymptotic expansion which we obtained from the Lippmann-Schwinger equation.

Further, it should be noticed that in each case the decrease is by one power better than it follows from what we subtracted. This is because each second power disappears under the sum of color and polarization.

As already mentioned, it turns out that for $\nu = 0$ and for $\nu = 1$ there are bound states. They manifest themselves as poles of the logarithm of the Jost function and, as a consequence, of the functions $\mathcal{E}_0^f(k)$ and $\mathcal{E}^f(\nu, k)$. These functions are shown in Fig. 4.

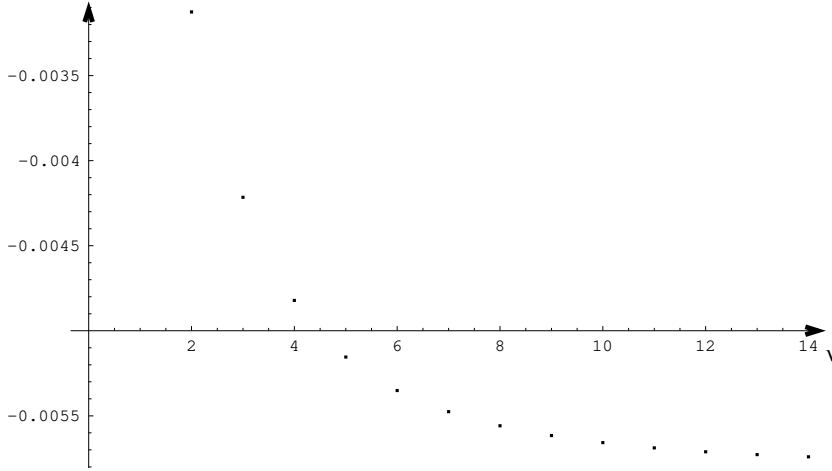


Figure 3: The contributions $\mathcal{E}^f(\nu)$ to the vacuum energy multiplied by ν^5 from the higher orbital momenta

4 The asymptotic part of the vacuum energy

Next we have to calculate the asymptotic contributions to the vacuum energy. Actually, the problem is to remove the auxiliary mass m and perform the analytic continuation to $s = 0$. We start with $\mathcal{E}_0^{\text{as}}$, Eq.(38) and insert there the asymptotic expansion (49). For $s > \frac{1}{2}$ we perform the limit $m \rightarrow 0$. The contribution from $\ln f_0^{\text{as}}(ik)$ which is proportional to $1/k$ vanishes. After that we can put $s = 0$ and are left with the finite integral

$$\int_0^\infty dk \, k^2 \frac{\partial}{\partial k} \frac{1}{(k^2 + 1)^{3/2}} = -2$$

and obtain

$$\mathcal{E}_0^{\text{as}} = \frac{1}{-8\pi} \sum_{c,\lambda} \int_0^\infty \frac{dr}{r} \left(\frac{P(r)}{16r^3} - \frac{P^2(r)}{8r^3} \right), \quad (65)$$

where $P(r)$ is given by Eq.(40). The sum over color and polarization can be carried out using (9) and (10),

$$\begin{aligned} \sum_{c,\lambda} 1 &= 2N, & \sum_{c,\lambda} \alpha_c^2 &= 2N, & \sum_{c,\lambda} \alpha_c^4 &= 4 \quad (\text{SU}(2)), \\ \sum_{c,\lambda} \alpha_c^4 &= 9/2 \quad (\text{SU}(3)), & \sum_{c,\lambda} \alpha_c^2 \left(\frac{1}{12} - \beta_\lambda^2 \right) &= \frac{-11N}{6}. \end{aligned} \quad (66)$$

We obtain

$$\mathcal{E}_0^{\text{as}} = \frac{N}{32\pi} \int_0^\infty \frac{dr}{r} \left(\mu^2(r) - \frac{N}{4} \mu^4(r) - 8r^2(\mu'(r))^2 \right) \quad (67)$$

for the s-wave contribution to the asymptotic part of the vacuum energy.

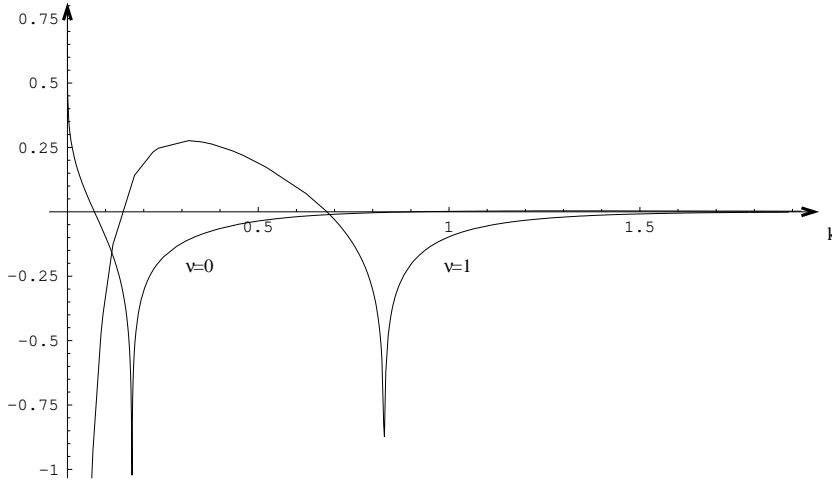


Figure 4: The functions $\mathcal{E}_0^f(k)$ and $\mathcal{E}^f(1, k)$ for small k . The poles indicate the positions of the bound states.

The contributions from the higher orbital momenta require more work. We start from rewriting \mathcal{E}^{as} , Eq.(35), using the Abel-Plana formula (see Appendix, Eq.(98)) in the form

$$\mathcal{E}^{\text{as}} = \sum_{c,\lambda} \left\{ \mathcal{E}^{\text{as}, \text{ a}} - \frac{1}{2} \mathcal{E}^{\text{as}, \text{ 0}} + \mathcal{E}^{\text{as}, \text{ b}} \right\} \quad (68)$$

with

$$\mathcal{E}^{\text{as}, \text{ a}} = \frac{C_s}{-4\pi} \int_0^\infty d\nu \int_m^\infty dk \ (k^2 - m^2)^{1-s} \frac{\partial}{\partial k} \ln f_\nu^{(c,\lambda)\text{as}}(ik), \quad (69)$$

$$\mathcal{E}^{\text{as}, \text{ 0}} = \frac{C_s}{-4\pi} \lim_{\nu \rightarrow 0} \int_m^\infty dk \ (k^2 - m^2)^{1-s} \frac{\partial}{\partial k} \ln f_\nu^{(c,\lambda)\text{as}}(ik), \quad (70)$$

$$\begin{aligned} \mathcal{E}^{\text{as}, \text{ b}} = & \frac{C_s}{-4\pi} \int_0^\infty \frac{d\nu}{1 - e^{2\pi\nu}} \int_m^\infty dk \ (k^2 - m^2)^{1-s} \frac{\partial}{\partial k} \\ & \times \frac{1}{i} \left(\ln f_{(iv)}^{(c,\lambda)\text{as}}(ik) - (\text{c.c.}) \right), \end{aligned} \quad (71)$$

where (c.c.) denotes complex conjugate. It should be noticed that $f_\nu^{(c,\lambda)\text{as}}(ik)$ is real so that (c.c.) changes in fact the sign of iv only. In Eq.(68) a factor of 2 from the negative orbital momenta was taken into account. The contribution from $\nu = 0$ deserves a remark. In fact, Eq.(98) is valid for a finite $f(0)$ only. This is ensured in our case by the auxiliary mass m . So we have first to perform the limes $\nu \rightarrow 0$. After that the limit $m \rightarrow 0$ produces from $\mathcal{E}^{\text{as}, \text{ 0}}$ a divergent contribution proportional to $1/m$ which is, however, canceled by a corresponding contribution from $\mathcal{E}^{\text{as}, \text{ b}}$.

Now we use the uniform asymptotic expansion of the logarithm of the Jost function as given by Eq.(44). So we insert it into $\mathcal{E}^{\text{as, a}}$ and interchange the orders of integration. For each contribution of the sum over n and j we use formula (100) given in the Appendix and obtain the representation

$$\mathcal{E}^{\text{as, a}} = \frac{1 + s(2 \ln 2 - 1)}{8\pi} m^{-2s} \Gamma(2 - s) \Gamma(s) \int_0^\infty \frac{dr}{r^3} \sum_{c,\lambda} \sum_{j=3}^7 \frac{Z_{3j}}{\frac{j}{2} - 1}, \quad (72)$$

where contributions proportional to powers of m are dropped. From Eqs. (97) and (66) we obtain

$$\sum_{c,\lambda} \sum_{j=3}^7 \frac{Z_{3j}}{\frac{j}{2} - 1} = \frac{-11N}{6} (r\mu'(r))^2. \quad (73)$$

In the limit $s \rightarrow 0$, $\mathcal{E}^{\text{as, a}}$ takes the form

$$\mathcal{E}^{\text{as, a}} = \frac{-11N}{48\pi^2} A \left(\frac{1}{s} + 2 \ln 2 - 1 - \gamma - 2 \ln m + O(s) \right) \quad (74)$$

with A given by Eq.(26).

Next contribution to be considered is $\mathcal{E}^{\text{as, 0}}$, Eq.(70). We insert $\ln f_\nu^{\text{as}}(ik)$ from Eq.(44) and use formula (99) from the Appendix,

$$\begin{aligned} \mathcal{E}^{\text{as, 0}} &= \frac{C_s}{4\pi} \lim_{\nu \rightarrow 0} \int_0^\infty \frac{dr}{r} \sum_{c,\lambda} \sum_{n=1}^3 \sum_{j=3n}^{3n} Z_{nj} \\ &\quad \times \frac{\Gamma(2 - s)\Gamma(s + \frac{j}{2} - 1)}{(mr)^j \Gamma(\frac{j}{2})} \frac{m^{2-2s} (\nu)^{j-n}}{\left(1 + \left(\frac{\nu}{mr}\right)^2\right)^{s+\frac{j}{2}-1}}. \end{aligned} \quad (75)$$

Here in the limes $\nu \rightarrow 0$ only contributions with $j = \nu$ remain (note $j \geq n$ in Eq.(42)). After that we consider the limits $m \rightarrow 0$ and $s = 0$. We obtain

$$\mathcal{E}^{\text{as, 0}} = \frac{1}{2\pi m} \int_0^\infty \frac{dr}{r^4} \sum_{c,\lambda} Z_{33} + O(m). \quad (76)$$

The contribution from $n = 2$ is odd under $\beta_\lambda \rightarrow -\beta_\lambda$ and does not contribute.

It remains to consider $\mathcal{E}^{\text{as, b}}$, Eq.(71). Again, inserting $\ln f_\nu^{\text{as}}(ik)$ from Eq.(44) and using formula (99) from the Appendix,

$$\begin{aligned} \mathcal{E}^{\text{as, b}} &= \frac{C_s}{4\pi} \int_m^\infty dk (k^2 - m^2)^{1-s} \frac{\partial}{\partial k} \int_0^\infty \frac{dr}{r} \sum_{n=1}^3 \sum_{j=n}^{3n} Z_{nj} \\ &\quad \times m^{2-2s} \frac{\Gamma(2 - s)\Gamma(s + \frac{j}{2} - 1)}{(mr)^j \Gamma(\frac{j}{2})} \Sigma_{nj}(mr) \end{aligned} \quad (77)$$

with the notation

$$\Sigma_{nj}(x) = \int_0^\infty \frac{d\nu}{1 - e^{2\pi\nu}} \frac{1}{i} \left[\frac{(i\nu)^{j-n}}{\left(\left(\frac{i\nu}{x}\right)^2 + 1\right)^{s+j/2-1}} - (\text{c.c.}) \right] \quad (78)$$

holds. In $\Sigma_{nj}(x)$ there is in fact no contribution from $\nu \leq x$ because $j - n$ is even. It can be rewritten in the form

$$\Sigma_{nj}(x) = \int_x^\infty \frac{d\nu}{1 - e^{2\pi\nu}} \frac{(-1)^{(n-1)/2} \cos \pi s \nu^{j-n}}{\left(\left(\frac{\nu}{x}\right)^2 - 1\right)^{s+j/2-1}}. \quad (79)$$

We have to perform the analytic continuation to $s = 0$. For $n = j = 1$ we simply can put $s = 0$ and obtain for small x (this is because we need $m \rightarrow 0$)

$$\Sigma_{11}(x) = \frac{-1}{12x} + O(x). \quad (80)$$

For $n = j = 3$ we also can put $s = 0$ and obtain

$$\Sigma_{33}(x) = x \int_x^\infty \frac{d\nu}{1 - e^{2\pi\nu}} \frac{1}{\sqrt{\nu^2 - x^2}}. \quad (81)$$

This integral is convergent. But for $x \rightarrow 0$ this form is not convenient. So we integrate two times by parts. We obtain first

$$\Sigma_{33}(x) = \frac{-\pi x}{1 - e^{2\pi x}} - 2 \int_x^\infty d\nu \arctan \frac{x}{\sqrt{\nu^2 - x^2}} \left(\frac{\nu}{1 - e^{2\pi\nu}} \right)' \quad (82)$$

and subsequently

$$\begin{aligned} \Sigma_{33}(x) &= \frac{-\pi x}{1 - e^{2\pi x}} + x \left(\pi + 2 \ln 2x^2 \right) \left(\frac{x}{1 - e^{2\pi x}} \right)' \\ &+ 2 \int_x^\infty d\nu \left[\nu \arctan \frac{x}{\sqrt{\nu^2 - x^2}} + x \left(\ln 2x + \ln \left(\nu + \sqrt{\nu^2 - x^2} \right) \right) \right] \left(\frac{\nu}{1 - e^{2\pi\nu}} \right)'' \end{aligned} \quad (83)$$

Here we can tend x to zero under the sign of the integral and arrive at

$$\Sigma_{33}(x) = \frac{1}{2} + x (\ln x + \Sigma_3) + O(x^2) \quad (84)$$

with

$$\Sigma_3 \equiv -1 + 2 \int_0^\infty d\nu \ln(2\nu) \left(\frac{\nu}{1 - e^{2\pi\nu}} \right)'' = -1.36437. \quad (85)$$

For $n = 3, j = 5$ we proceed in a similar way. In order to perform the analytic continuation to $s = 0$ we integrate by parts and obtain

$$\Sigma_{35}(x) = -2x^3 \int_x^\infty \frac{d\nu}{\sqrt{\nu^2 - x^2}} \left(\frac{\nu}{1 - e^{2\pi\nu}} \right)'. \quad (86)$$

For $x \rightarrow 0$ we have to integrate by parts once more and get

$$\Sigma_{35}(x) = x^3 (\ln x + \Sigma_5) + O(x^4) \quad (87)$$

with

$$\Sigma_5 \equiv 2 \int_0^\infty d\nu \ln(2\nu) \left(\frac{\nu}{1 - e^{2\pi\nu}} \right)'' = -0.364378. \quad (88)$$

Finally we have $n = 3, j = 7$. For $s = 0$ we integrate two times by parts and obtain

$$\Sigma_{37}(x) = -\frac{2}{3}x^5 \int_x^\infty \frac{d\nu}{\sqrt{\nu^2 - x^2}} \left(\frac{1}{\nu} \left(\frac{\nu^3}{1 - e^{2\pi\nu}} \right)' \right)' . \quad (89)$$

For $x \rightarrow 0$ we have to integrate by parts once more and get

$$\Sigma_{37}(x) = x^5 (\ln x + \Sigma_7) + O(x^6) \quad (90)$$

with

$$\Sigma_7 = \frac{2}{3} \int_0^\infty d\nu \ln(2\nu) \left(\frac{1}{\nu} \left(\frac{\nu^3}{1 - e^{2\pi\nu}} \right)' \right)'' = -0.121459. \quad (91)$$

Having now the appropriate representations for Σ_{nj} we can insert them into $\mathcal{E}^{\text{as, b}}$, Eq.(77). We start from considering $n = j = 1$. Inserting (80) we obtain

$$\mathcal{E}^{\text{as, b}(11)} = \frac{N}{48\pi} \int_0^\infty \frac{dr}{r^2} \mu(r) \mu'(r). \quad (92)$$

Next we look for the first contribution in the rhs. of Eq.(84). It gives a contribution to $\mathcal{E}^{\text{as, b}}$, Eq.(77) which is proportional to $1/m$ and it cancels just the contribution of $\mathcal{E}^{\text{as, 0}}$, Eq.(76). Next we consider contributions from Σ_{3j} containing the logarithm $\ln(rm)$. What is proportional to $\ln m$ can be seen to cancel exactly the corresponding contribution from $\mathcal{E}^{\text{as, a}}$, Eq.(74). The remaining part is

$$\mathcal{E}^{\text{as, b}(\ln)} = \frac{-11N}{24\pi} \int_0^\infty \frac{dr}{r} \ln r \mu'(r)^2. \quad (93)$$

Finally we collect the contributions from Σ_j and denote them $\mathcal{E}^{\text{as, b}(3j)}$ ($j = 3, 5, 7$). They read explicitly

$$\mathcal{E}^{\text{as, b}(3j)} = \frac{1}{4\pi} \int_0^\infty \frac{dr}{r^3} \sum_{c,\lambda} \sum_j \frac{Z_{3j}}{j/2 - 1} \Sigma_j \quad (94)$$

with Z_{3j} given by Eqs.(97). Performing the sum over color and polarization we obtain

$$\begin{aligned} \mathcal{E}^{\text{as, b}(33)} &= \frac{N\Sigma_3}{24\pi} \int_0^\infty \frac{dr}{r^2} \left(-11\mu(r)\mu'(r) + 6r\mu(r)\mu''(r) - 6r(\mu'(r))^2 \right. \\ &\quad \left. - \frac{N}{2}\mu^3(r)\mu'(r) \right), \end{aligned}$$

$$\begin{aligned}
\mathcal{E}^{\text{as, b(35)}} &= \frac{N\Sigma_5}{24\pi} \int_0^\infty \frac{dr}{r^2} \left(26\mu(r)\mu'(r) - 6r\mu(r)\mu''(r) - 5r(\mu'(r))^2 \right. \\
&\quad \left. + N\mu^3(r)\mu'(r) \right), \\
\mathcal{E}^{\text{as, b(37)}} &= \frac{-5N\Sigma_7}{16\pi} \int_0^\infty \frac{dr}{r^2} \mu(r)\mu'(r).
\end{aligned} \tag{95}$$

In this way the complete asymptotic part \mathcal{E}^{as} from the higher orbital momenta, Eq.(68), of the vacuum energy reads

$$\mathcal{E}^{\text{as}} = \mathcal{E}^{\text{as, b(11)}} + \mathcal{E}^{\text{as, b(ln)}} + \mathcal{E}^{\text{as, b(33)}} + \mathcal{E}^{\text{as, b(35)}} + \mathcal{E}^{\text{as, b(37)}}, \tag{96}$$

where the individual parts are given by Eqs. (92), (93) and (95).

$\mu(r)$	$\nu = 0$	$\nu = 1$
$\tanh^2 r$	$\kappa_0 = 0.82862$	$\kappa_1 = 0.16771$
$\tanh^4 r$	$\kappa_0 = 0.58388$	$\kappa_1 = 0.16379$
$\tanh^8 r$	$\kappa_0 = 0.46125$	$\kappa_1 = 0.15486$
$r^6/(1+r^6)$	$\kappa_0 = 0.742808$	$\kappa_1 = 0.28539$

Table 1: The bound state levels κ in Eq.(16).

5 Numerical Results

The actual calculation have been performed for four profiles $\mu(r)$, see for example Table 1, using Mathematica. For the solution of the differential equation (55) the build in function `NDSolve` had been used. The working precision was taken to be 25 digits and the pure computation time was about 40 hours on a standard PC. The good convergence of the integrals and of the sums was already discussed in Sect. 3. The numerical integrations had been done with the build in function which calculated about 200 points for each integral. In this way the numerical effort is not very demanding.

In the examples considered here there are bound states in the spectrum of the fluctuations. They result in an imaginary part in the vacuum energy, see Eq.(16). In the subdivision of the vacuum energy according to Eq.(33) the imaginary part resides in the finite parts, \mathcal{E}_0^f and \mathcal{E}^f . Thereby the first bound state appears in the s-wave contribution \mathcal{E}_0^f , the second in the p-wave ($\nu = 1$). The binding energies are shown in Table 1. These bound states do not depend on the gauge group $SU(2)$ or $SU(3)$ because they come from the color eigenvalues $\alpha_c = \pm 1$ in Eq.(9) which are common to both groups.

In Table 2 the numerical results for the asymptotic parts of the vacuum energy \mathcal{E}^{as} , Eq.(35) are shown. It is seen that $\mathcal{E}^{\text{as, b(33)}}$ is the numerically dominating

N	$\mathcal{E}^{\text{as, b(11)}}$	$\mathcal{E}^{\text{as, b(ln)}}$	$\mathcal{E}^{\text{as, b(33)}}$	$\mathcal{E}^{\text{as, b(35)}}$	$\mathcal{E}^{\text{as, b(37)}}$	\mathcal{E}^{as}
$\mu(r) = \tanh^2 r$						
2	0.00823767	0.16906	0.507441	-0.138928	0.0150082	0.208057
3	0.0123565	0.25359	0.753783	-0.204451	0.0225122	0.311155
$\mu(r) = \tanh^4 r$						
2	0.00360497	0.00354893	0.272918	-0.0634807	0.00656787	0.138266
3	0.00540745	0.00532339	0.405012	-0.0928895	0.00985181	0.2064
$\mu(r) = \tanh^8 r$						
2	0.00213291	-0.0326859	0.190348	-0.0386886	0.00388594	0.0825228
3	0.00319937	-0.0490288	0.282582	-0.0564628	0.00582891	0.122963
$\mu(r) = r^6/(1 + r^6)$						
2	0.00534584	0.0228004	0.561348	-0.0998484	0.00973955	0.310584
3	0.00801875	0.0342006	0.833918	-0.145444	0.0146093	0.464541

Table 2: The constituents of the asymptotic part \mathcal{E}^{as} of the vacuum energy according to Eq.(96).

contribution. Within it the dominating part is $(\mu'(r))^2$ over weighting that of $(\mu(r))^2$. Therefore there seems to be no chance to change the sign of $\mathcal{E}^{\text{as, b(33)}}$ taking another profile function $\mu(r)$.

In Table 3 the numerical results for the vacuum energy $\mathcal{E}_{\text{quant}}^{\text{renPV}}$ given by Eq.(33) are shown. The dominating part is the asymptotic contribution \mathcal{E}^{as} , followed by $\mathcal{E}_0^{\text{as}}$. The finite contributions \mathcal{E}^{f} and \mathcal{E}_0^{f} are considerably smaller.

We conclude the representation of the numerical results by Table 4 showing the quantities entering the calculation of the minimum of the complete energy, namely A , Eq.(26), B , Eq.(28), the radius $r_0|_{\text{min}}$, Eq.(30) and the energy in the minimum, $\mathcal{E}|_{\text{min}}$, Eq.(31) (the latter two quantities are given in units of Λ_{QCD}).

6 Conclusions

We calculated the vacuum energy for a color magnetic vortex in QCD. We found that the renormalized vacuum energy $\mathcal{E}_{\text{quant}}^{\text{renPV}}$ calculated at $r_0 = 1$ is positive. As discussed in Sec. 2 the sign of the complete energy in the minimum $\mathcal{E}|_{\text{min}}$, Eq.(31), is not affected by this sign but only its deepness. For a positive $\mathcal{E}_{\text{quant}}^{\text{renPV}}$ it is less deep. At once the core radius becomes larger. In this sense $\mu(r) = \tanh^8 r$ is the 'best' one among the considered profile functions.

In general, the sign of the vacuum energy is hard to predict. In the given case the vacuum energy $\mathcal{E}_{\text{quant}}^{\text{renPV}}|_{r_0=1}$ which is positive results from bosonic fluctuations whereas in the magnetic background calculated in [6, 21, 4] it is negative resulting

N	$\mathcal{E}_0^{\text{as}}$	$\mathcal{E}_0^{\text{as}}$	\mathcal{E}_0^{f}	\mathcal{E}^{f}	$\mathcal{E}_{\text{quant}}^{\text{renPV}}$
$\mu(r) = \tanh^2 r$					
2	-0.352761	0.560818	-0.0482214	-0.00659258	0.153243
3	-0.526636	0.83779	-0.0894967	0.00379912	0.273678
$\mu(r) = \tanh^4 r$					
2	-0.0848931	0.223159	-0.0889963	0.000655135	0.0499246
3	-0.126305	0.332705	-0.12675	0.0101892	0.178836
$\mu(r) = \tanh^8 r$					
2	-0.0424693	0.124992	-0.0649512	0.00630883	0.0238805
3	-0.0631556	0.186119	-0.0903911	0.0161882	0.113711
$\mu(r) = r^6/(1 + r^6)$					
2	-0.188802	0.499386	-0.08936	0.0452825	0.266506
3	-0.280762	0.745303	-0.137446	0.0877988	0.504254

Table 3: The constituents of the vacuum energy according to Eq.(33).

from fermionic ones. However, these results cannot be compared directly because of different normalization conditions used (massless vs. massive case). Nevertheless, one may wonder to what extend this is a general rule and what the quark contributions might change for a center-of-group vortex.

The topic of stability of the vortex is to a large extend beyond the scope of the present paper. So we only remark that the bound states and the imaginary part found here make the whole configuration unstable with respect to creation of particles. This is the same instability as known from the homogenous color magnetic field.

The bound states are well known in a homogeneous color magnetic field. In an inhomogeneous one their existence can be predicted from some simple arguments. First note that the background we are concerned with is in fact Abelian and the contribution proportional to $\mu'(r)$ in Eq.(8) is an additional magnetic moment. From [22] it is known that for a balance between the lowest Landau level and an attractive interaction between the magnetic moment and the magnetic background field there are zero modes, one for each flux quantum. In [22] this had been established for an electron but it is obvious that this holds in our case too. Here the magnetic moment is larger due to the spin of the gluon. The zero modes become more tightly bounded and turn into bound states. This is independent from the specific form of the background and it is what we observed for our profile functions $\mu(r)$. The bound states found here are also in line with those in [23] where an electron with gyromagnetic factor larger than 2 had been considered.

N	A	B	$r_0 _{\min} \Lambda_{\text{QCD}}$	$\mathcal{E}_{ _{\min}}/\Lambda_{\text{QCD}}^2$
$\mu(r) = \tanh^2 r$				
2	0.864328	0.148238	11.1221	-0.000324477
3	0.864328	0.103024	16.0032	-0.000235092
$\mu(r) = \tanh^4 r$				
2	0.488359	0.332642	4.95644	-0.000923169
3	0.488359	0.072185	22.8402	-0.0000652096
$\mu(r) = \tanh^8 r$				
2	0.353234	0.482925	3.41403	-0.00140737
3	0.353234	0.0991947	16.6211	-0.0000890673
$\mu(r) = r^6/(1+r^6)$				
2	1.07484	0.0692783	23.7985	-0.0000881308
3	1.07484	0.0344776	47.8201	-0.0000327415

Table 4: Summary for the energy of the vortex

The calculations had been performed in an efficient way, using Jost functions and separating an asymptotic part thus leaving fast convergent expressions. The main numerical effort is for the finite parts. Here one has to perform the integration over the radial momentum and the sum over the orbital momenta which are fast converging due to the subtraction of the corresponding first few terms of the asymptotic expansions. For instance, in Eq.(57) we subtract up to $O\left(\frac{1}{\nu^3}\right)$ which is sufficient for convergence. It turns out that the next power, $\frac{1}{\nu^4}$ is absent and we are left with an $\frac{1}{\nu^5}$ -behavior making the sum in Eq.(57) fast convergent. The absence of the $\frac{1}{\nu^4}$ -contribution is due to cancellations between the orbital momenta of different sign⁴. Furthermore, this cancellation is related to the smoothness properties of the background. If the background has a jump, as, for instance, considered in [6, 24, 21], a contribution proportional to $\frac{1}{\nu^4}$ is present slowing down the convergence. Of course, one may think about over subtractions, i.e., including more terms in the asymptotic part of the Jost function, Eq.(42). But there one needs more orders in the iteration of the Lippmann-Schwinger equation than done in [6]. This had been done only for the particular example of the pure magnetic background in [24].

In Sec. 5 it was found that the numerically dominating contribution results from \mathcal{E}^{as} . It is of some interest to discuss the question whether \mathcal{E}^{as} can be attributed to a orbital momentum. We start with the remark that the initial, regularized vacuum energy $\mathcal{E}_{\text{quant}}$, (11), which appears after separation of vari-

⁴We note that this had been taken into account in the coefficients X_{nj} and Z_{nj} which are listed in the Appendix.

ables, is a sum over orbital momenta. This remains true also after the subdivision into finite and asymptotic parts in Sec. 3 and for the finite parts themselves. Also $\mathcal{E}_0^{\text{as}}$ can be attributed to the s-wave. However, \mathcal{E}^{as} cannot. Here the reason is that in order to perform the analytic continuation to $s = 0$ we used the Abel-Plana formula and performed the integration over ν after what it is impossible to identify contributions from some ν . In this way we cannot say from which orbital momentum the numerically dominating contribution originates. To some extend this discussion can be continued with the remark that it is the counter term who cannot be represented as a sum over orbital momenta.

Acknowledgments

The author is indebted to D. Diakonov for directing his attention to this problem and for interesting discussions during a very pleasant visit to Copenhagen. The author thanks K. Kirsten, H. Gies, V. Skalozub and D. Vassilevich for interesting and helpful discussions.

Appendix

The coefficients X_{nj} appearing in Eq.(42) read

$$\begin{aligned}
X_{1,1} &= \frac{\alpha_c^2 \mu(r)^2}{2}, \\
X_{1,2} &= 0, \\
X_{1,3} &= \frac{-\left(\alpha_c^2 \mu(r)^2\right)}{2}, \\
X_{2,2} &= \frac{\alpha_c^2 \mu(r)^2}{2} - \frac{\alpha_c^2 r \mu(r) \mu'(r)}{2}, \\
X_{2,3} &= -\left(\alpha_c^2 \beta_\lambda r \mu(r) \mu'(r)\right), \\
X_{2,4} &= \frac{-5 \alpha_c^2 \mu(r)^2}{2} + \alpha_c^2 r \mu(r) \mu'(r), \\
X_{2,5} &= 0, \\
X_{2,6} &= 2 \alpha_c^2 \mu(r)^2, \\
X_{3,3} &= \frac{13 \alpha_c^2 \mu(r)^2}{16} - \frac{\alpha_c^4 \mu(r)^4}{8} - \alpha_c^2 r \mu(r) \mu'(r) + \frac{\alpha_c^2 r^2 \mu'(r)^2}{4} \\
&\quad - \frac{\alpha_c^2 \beta_\lambda^2 r^2 \mu'(r)^2}{2} + \frac{\alpha_c^2 r^2 \mu(r) \mu''(r)}{4}, \\
X_{3,4} &= -3 \alpha_c^2 \beta_\lambda r \mu(r) \mu'(r) + \alpha_c^2 \beta_\lambda r^2 \mu'(r)^2 + \alpha_c^2 \beta_\lambda r^2 \mu(r) \mu''(r), \\
X_{3,5} &= \frac{-153 \alpha_c^2 \mu(r)^2}{16} + \frac{3 \alpha_c^4 \mu(r)^4}{4} + \frac{27 \alpha_c^2 r \mu(r) \mu'(r)}{4}
\end{aligned}$$

$$\begin{aligned}
& - \frac{5 \alpha_c^2 r^2 \mu'(r)^2}{8} - \frac{3 \alpha_c^2 r^2 \mu(r) \mu''(r)}{4}, \\
X_{3,6} &= 4 \alpha_c^2 \beta_\lambda r \mu(r) \mu'(r), \\
X_{3,7} &= \frac{315 \alpha_c^2 \mu(r)^2}{16} - \frac{5 \alpha_c^4 \mu(r)^4}{8} - \frac{25 \alpha_c^2 r \mu(r) \mu'(r)}{4}, \\
X_{3,8} &= 0, \\
X_{3,9} &= \frac{-175 \alpha_c^2 \mu(r)^2}{16}.
\end{aligned}$$

The non vanishing coefficients Z_{nj} appearing in Eq.(44) read

$$\begin{aligned}
Z_{1,1} &= \alpha^2 r \mu(r) \mu'(r), \\
Z_{2,3} &= -(\alpha^2 \beta r \mu(r) \mu'(r)), \\
Z_{3,3} &= \frac{-\left(\alpha^4 r \mu(r)^3 \mu'(r)\right)}{6} - \frac{\alpha^2 (-1 + 2 \beta^2) r^2 \mu'(r)^2}{4} \\
&\quad + \frac{\alpha^2 r \mu(r) (-11 \mu'(r) + 6 r \mu''(r))}{24}, \\
Z_{3,4} &= \alpha^2 \beta r^2 \mu'(r)^2 + \alpha^2 \beta r \mu(r) (-3 \mu'(r) + r \mu''(r)), \\
Z_{3,5} &= \frac{\alpha^4 r \mu(r)^3 \mu'(r)}{2} - \frac{5 \alpha^2 r^2 \mu'(r)^2}{8} - \frac{\alpha^2 r \mu(r) (-13 \mu'(r) + 3 r \mu''(r))}{4}, \\
Z_{3,6} &= 4 \alpha^2 \beta r \mu(r) \mu'(r), \\
Z_{3,7} &= \frac{-25 \alpha^2 r \mu(r) \mu'(r)}{8}.
\end{aligned} \tag{97}$$

The Abel-Plana formula used in Sect.2 reads

$$\sum_{\nu=1}^{\infty} f(\nu) = \int_0^{\infty} d\nu f(\nu) - \frac{1}{2} f(0) + \int_0^{\infty} \frac{d\nu}{1 - e^{2\pi\nu}} \frac{f(i\nu) - f(-i\nu)}{i}. \tag{98}$$

The following formulas are used in the text,

$$\int_m^{\infty} dk (k^2 - m^2)^{1-s} \frac{\partial}{\partial k} t^j = -m^{2-2s} \frac{\Gamma(2-s) \Gamma(s + \frac{j}{2} - 1)}{\Gamma(\frac{j}{2})} \frac{\left(\frac{\nu}{mr}\right)^{j-n}}{\left(1 + \left(\frac{\nu}{mr}\right)^2\right)^{s+\frac{j}{2}-1}} \tag{99}$$

and

$$\int_0^{\infty} d\nu \int_m^{\infty} dk (k^2 - m^2)^{1-s} \frac{\partial}{\partial k} \frac{t^j}{\nu^n} = -\frac{m^{2-2s}}{2(rm)^{n-1}} \frac{\Gamma(2-s) \Gamma(\frac{1+j-n}{2}) \Gamma(s + \frac{n-3}{2})}{\Gamma(j/2)} \tag{100}$$

with $t = 1/\sqrt{1 + (kr/\nu)^2}$. They can be easily derived, see also (C3) and (C2) in [6].

References

- [1] Gerard 't Hooft. On the phase transition towards permanent quark confinement. *Nucl. Phys.*, B138:1, 1978.
- [2] L. Del Debbio, M. Faber, J. Greensite, and S. Olejnik. Center dominance and $Z(2)$ vortices in $SU(2)$ lattice gauge theory. *Phys. Rev.*, D55:2298–2306, 1997.
- [3] M. Engelhardt and H. Reinhardt. Center vortex model for the infrared sector of Yang-Mills theory: Confinement and deconfinement. *Nucl. Phys.*, B585:591–613, 2000.
- [4] Kurt Langfeld, Laurent Moyaerts, and Holger Gies. Fermion-induced quantum action of vortex systems. 2002. hep-th/0205304.
- [5] Dmitri Diakonov and Martin Maul. Center-vortex solutions of the Yang-Mills effective action in three and four dimensions. 2002. hep-lat/0204012.
- [6] M. Bordag and K. Kirsten. The Ground state energy of a spinor field in the background of a finite radius flux tube. *Phys. Rev.*, 60:105019, 1999.
- [7] M. Bordag and K. Kirsten. Vacuum energy in a spherically symmetric background field. *Phys. Rev.*, D53:5753–5760, 1996.
- [8] Noah Graham, Robert L. Jaffe, and Herbert Weigel. Casimir effects in renormalizable quantum field theories. *Int. J. Mod. Phys.*, A17:846–869, 2002.
- [9] Klaus Kirsten. *Spectral functions in mathematics and physics*. Chapman & Hall/CRC, Boca Raton, FL, 2001.
- [10] Holger Gies and Kurt Langfeld. Loops and loop clouds: A numerical approach to the worldline formalism in QED. *Int. J. Mod. Phys.*, A17:966–978, 2002.
- [11] Holger Gies and Kurt Langfeld. Quantum diffusion of magnetic fields in a numerical worldline approach. *Nucl. Phys.*, B613:353–365, 2001.
- [12] Pavlos Pasipoularides. Fermion-induced effective action in the presence of a static inhomogeneous magnetic field. *Phys. Rev.*, D64:105011, 2001.
- [13] M. Bordag. Ground state energy for massive fields and renormalization. *Comments on Atomic and Nuclear Physics, Comments on Modern Physics*, 1, part D:347–361, 2000.
- [14] M. Bordag, K. Kirsten, and D. Vassilevich. On the ground state energy for a penetrable sphere and for a dielectric ball. *Phys. Rev.*, D59:085011, 1999.

- [15] M. Bordag, E. Elizalde, K. Kirsten, and S. Leseduarte. Casimir energies for massive fields in the bag. *Phys. Rev.*, D56:4896–4904, 1997.
- [16] Michael Bordag, Alfred Scharff Goldhaber, Peter van Nieuwenhuizen, and Dmitri Vassilevich. Heat kernels and zeta-function regularization for the mass of the susy kink. hep-th/0203066, 2002.
- [17] B.S. DeWitt. *The Dynamical Theory of Groups and Fields*. Gordon and Breach, New York, 1965.
- [18] M. Bordag. Vacuum energy in smooth background fields. *J. Phys.*, A28:755–766, 1995.
- [19] Michael Bordag, Meik Hellmund, and Klaus Kirsten. Dependence of the vacuum energy on spherically symmetric background fields. *Phys. Rev.*, D 61:085008, 2000.
- [20] E. Elizalde, M. Bordag, and K. Kirsten. Casimir energy for a massive fermionic quantum field with a spherical boundary. *J. Phys. A*, A31:1743, 1998.
- [21] Martin Groves and Warren B. Perkins. The Dirac sea contribution to the energy of an electroweak string. *Nucl. Phys.*, B573:449–500, 2000.
- [22] Y. Aharonov and A. Casher. Ground state of a spin-1/2 charged particle in a two-dimensional magnetic field. *Phys. Rev.*, A19:2461–2462, 1979.
- [23] M. Bordag and S. Voropaev. Bound states and scattering of an electron in the field of the magnetic string. *Phys. Lett.*, B333:238, 1994.
- [24] I. Drozdov. Vacuum polarization by a magnetic flux of special rectangular form. 2002. hep-th/0210282.